ChemComm
Chemical Communications

Accepted Manuscript

This article can be cited before page numbers have been issued, to do this please use: F. Santos, F. G. Blandón-Cumbreras, U. Pischel and P. P. Gois, *Chem. Commun.*, 2026, DOI: 10.1039/D6CC00206D.

ROYAL SOCIETY OF CHEMISTRY

rsc.li/chemcomm

View Article Online
DOI: 10.1039/D6CC00206D

BASHY dyes as modular chromophores for multifaceted biorelevant applications: From imaging to photodynamic therapy

Fábio M. F. Santos,*[a] Francisco G. Blandón-Cumbreras,[b] Uwe Pischel*[b] and Pedro M. P. Gois*[a]

[a] *Research Institute for Medicines (iMed.ULisboa), Faculty of Pharmacy, Universidade de Lisboa, Lisbon 1649-003, Portugal*

[b] *CIQSO – Centre for Research in Sustainable Chemistry and Department of Chemistry, University of Huelva, Campus de El Carmen, E-21071 Huelva, Spain*

View Article Online
DOI: 10.1039/D6CC00206D

Abstract

The multifactorial nature of biological systems and the ongoing effort to elucidate their underlying mechanisms have driven the demand for advanced fluorescent probes with high sensitivity and functional adaptability. To meet these challenges, multicomponent reactions (MCRs) offer a powerful synthetic strategy for the straightforward design of structurally diverse fluorophores with tunable chemical and photophysical properties. In this context, the boronic-acid derived salicylidenehydrazone (BASHY) platform has emerged as a versatile class of dyes featuring π-conjugated ligands coordinated to an sp^3-hybridized boron centre. This molecular design yields fluorophores with polarity-sensitive emission and significant photostability. The modular scaffold allows the systematic tuning of photophysical properties, while preserving fluorescence efficiency upon derivatization.

BASHY dyes display exceptional performance in bioimaging, enabling the labeling of lipid droplets (LDs), astrocytes, apoptotic cells, and myelin debris in *in vivo* demyelination models. The BASHY framework also supports energy-transfer cassettes (ETCs) with nearly quantitative energy transfer efficiencies and offers compatibility with fluorescence lifetime imaging microscopy (FLIM). Beyond imaging, BASHY dyes act as highly efficient singlet-oxygen photosensitizers (PS) with application potential in photodynamic therapy (PDT). Furthermore, specifically designed conjugates integrate both imaging and therapeutic functions, displaying potent cytotoxicity.

In this review, we discuss the evolution of the BASHY platform and its applications that positions these dyes as promising candidates for next-generation imaging and theranostic agents.

View Article Online
DOI: 10.1039/D6CC00206D

View Article Online
DOI: 10.1039/D6CC00206D

Introduction

Fluorescent dyes are an invaluable class of functional molecules, widely used to study the intricacies of biological processes. In recent years, considerable efforts have been made to expand the chemical space of these compounds by designing chromophores with structural and photophysical properties that are tailored for bioimaging.[1–18]

Several classes of small organic frameworks, such as coumarins, naphthalimides, fluoresceins, rhodamines, BODIPY or cyanines, (**Figure 1**) have gained prominence in this field, mainly due to their suitable biocompatibility and exceptional photophysical properties, including high photostability, brightness, and quantum yields. Owing to these properties, these dyes have been widely used to enhance our ability to visualize and follow complex biological processes with high sensitivity and specificity.[19,20]

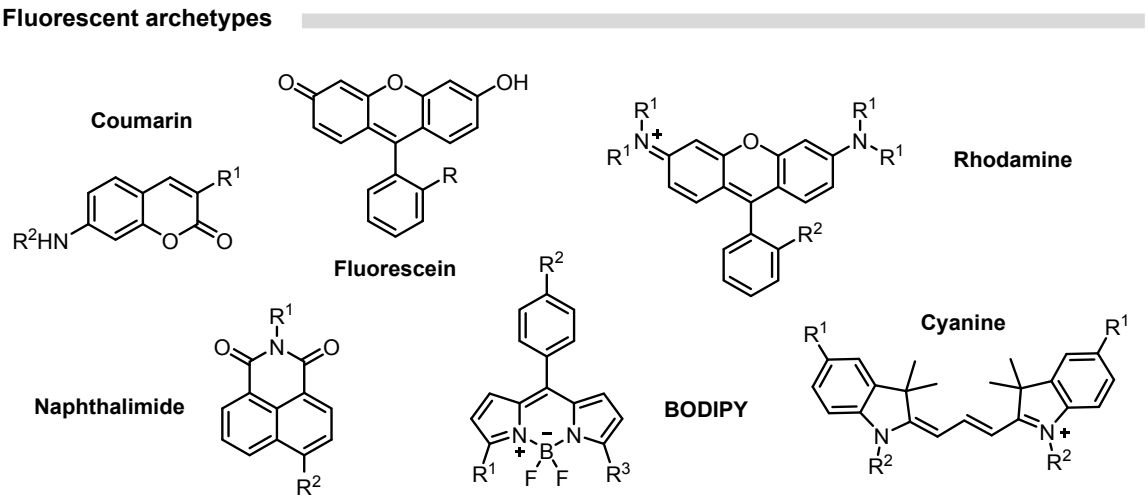

Figure 1. Representative fluorescent frameworks employed in bioimaging.

However, the use of these dyes in specific applications often requires the adaptation of the chromophore architecture to meet concrete biological

View Article Online
DOI: 10.1039/D6CC00206D

requirements. This task is particularly challenging, because molecular diversification can affect the electronic structure and consequently the photophysical properties of the chromophore. Therefore, the development of synthetic methods to create easily tuneable dyes with predictable fluorescence properties is critical to advancing the imaging of complex biological processes.

The high structural diversity offered by multicomponent reactions (MCRs) can be a particularly useful strategy, either for the diversification of functional fluorescent molecules (scaffold approach) or for the discovery of novel π-conjugated frameworks (chromogenic approach). Müller and co-workers have comprehensively reviewed this subject, showcasing various examples of valuable MCRs, including Ugi, Biginelli, Debus-Radziszwski, Groebke-Blackburn-Bienaymé (GBB), among others (**Figure 2A**).[21,22] One noteworthy example of a powerful application of MCRs in chromophore synthesis was the development of PyrAtes by Maulide and co-workers in 2024. This novel fluorophore class features an imidazo[1,2-*a*]pyridinium core, exhibiting remarkable photophysical properties and potential for live-cell imaging applications **(Figure 2B)**.[23] Despite some scattered successful examples, the current use of MCRs predominantly focuses on the structural diversification of existing chromophores. Only a limited number of MCRs have been reported to directly generate fluorescent cores with photophysical properties suitable for bioimaging applications.[22]

View Article Online
DOI: 10.1039/D6CC00206D

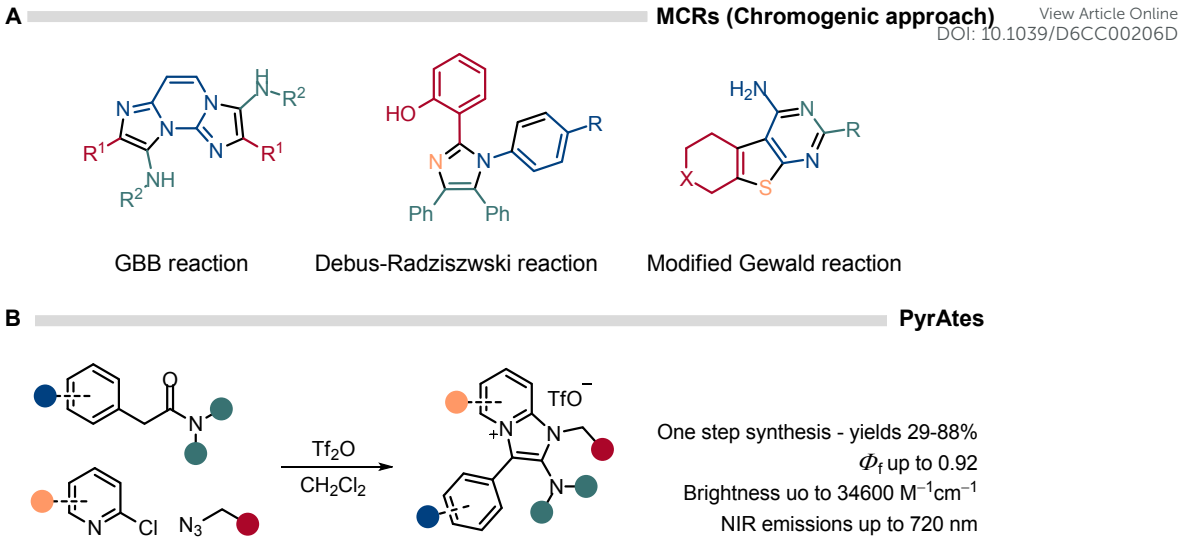

Figure 2. A) Selected examples of MCRs applied in discovery of novel π-conjugated systems; **B**) Multicomponent synthesis of PyrAtes and some of their photophysical properties.

Boron is a prevalent element in the structure of many chromophores and the success of the BODIPY dyes[24] led to the discovery of numerous fluorescent architectures with bidentate ligands tethered by a central boron atom that is coordinated to fluorine or aromatic anions. In many of these chromophores, the boron atom plays a crucial role in improving ligand stability, dye planarity, conjugation, and charge transfer throughout the π system.[25] However, boronic acids (BAs), one of the most versatile reagents in modern synthesis, have generally been overlooked as tethers for the construction of fluorescent dyes. This restricted applicability can be rationalized by the following factors: I) sp^2-hybridized boron complexes are highly reversible under aqueous conditions,[26] which may limit their suitability for advanced bioimaging applications; II) sp^3-hybridized boron complexes are known to be more stable,[27] however their tetrahedral geometry forces substituents out of the plane of conjugation,

View Article Online
DOI: 10.1039/D6CC00206D

potentially compromising the chromophores' photophysical characteristics (**Figure 3A**).[28,29]

BAs exhibit a very rich coordination chemistry,[30] are responsive to different physiological stimuli, and are readily available in a huge structural diversity, which has allowed the preparation of a plethora of materials for applications as diverse as sensing of carbohydrate[31–33] and anions[31,33,34], non-linear optics,[28,35–38] drug delivery[39] or the construction of biomaterials.[40,41] Encouraged by this functional and structural diversity, in 2016 we initiated a program to explore BAs as building blocks in MCRs for the construction of chromophores.[42] The motivation for this work was not only to gain access to the chemical space of dyes for bioimaging, but equally important, to design modular and responsive chromophores that can elucidate the intricacies of biological processes, critical to disease detection and monitoring.[43,44]

Unveiling and structural diversification of the BASHY platform

The discovery of BASHY dyes

Our aim was to design multicomponent chromophores using BAs as a component and conformational lock. Therefore, we established as a design principle, ligands with donor and acceptor groups, generating a π-conjugated system capable of coordinating the BA. To this end we investigated the coordination of Schiff-based ligands with BAs (**Figure 3B**). Unfortunately, the prepared boronates exhibited very poor photophysical properties, which was in accordance with earlier observations of Waksman and co-workers.[29] However, when the phenylglyoxylic acid was selected as the acceptor group, and bridged to the

View Article Online
DOI: 10.1039/D6CC00206D

donor group by a hydrazone function, a fluorescent BASHY was obtained in nearly quantitative yield (**Figure 3C**).[42]

It is noteworthy, that since the discovery of BASHY dyes, several multicomponent and fluorescent BA-based frameworks (**Figure 4**) have been developed, featuring red/near-infrared absorption,[45,46] solid-state fluorescence,[45–51] stimuli-responsive fluorescence,[47–49,52–56] and aggregation-induced emission.[50,54,57–59] These chromophores have also shown promising potential for cell bioimaging,[53] including the staining of lipid droplets (LDs),[51,58] lysosomes,[50] mitochondria,[45,46,50] and the endoplasmic reticulum.[49]

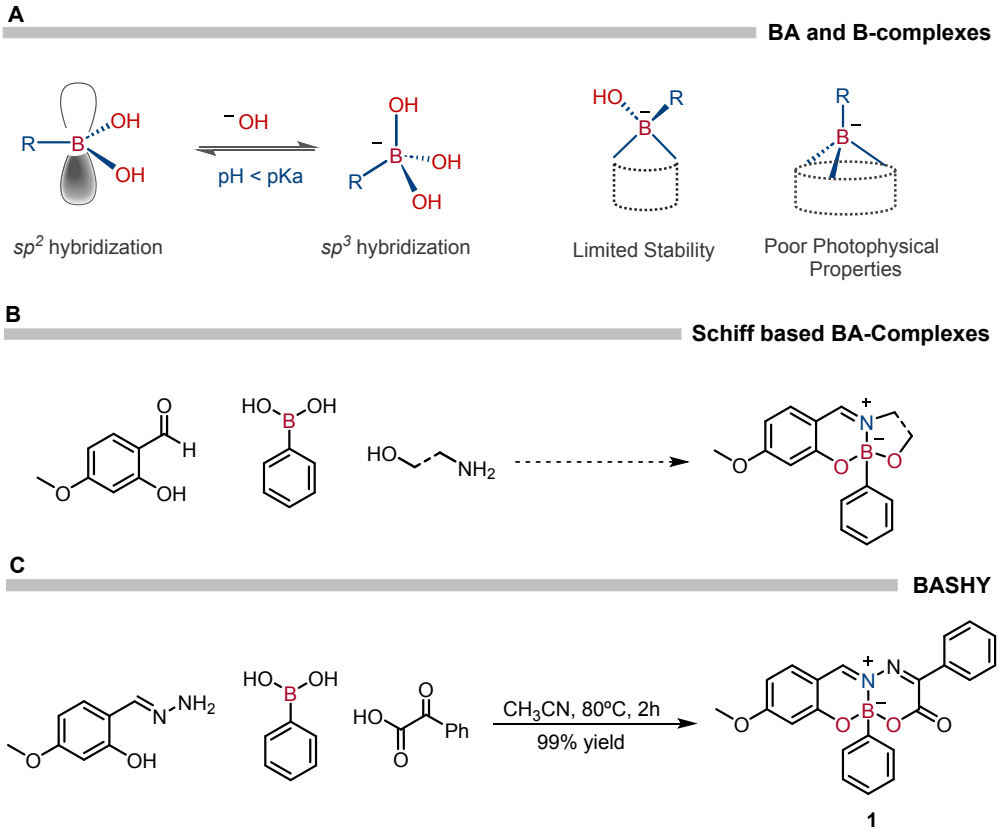

Figure 3. A) BA hybridization states and chelation with bi- and tri- dentate ligands; **B**) Schiff-base tetrahedral BA-complexes; **C**) Modular synthesis of BASHY dye **1**.

View Article Online
DOI: 10.1039/D6CC00206D

The photophysical evaluation of the first generation of BASHY dyes revealed a pronounced intramolecular charge-transfer (ICT) character with a polarity-sensitive green-to-yellow emission, high emission quantum yields (up to 0.6) in nonpolar environments, high brightness (up to 54000 $M^{-1}cm^{-1}$), large Stokes shifts (up to 100 nm), and a high photostability. In addition to these photophysical properties, the BASHY modular architecture offers various positions for structural diversification and optimization of the photophysical properties (**Figure 4**; moieties **A**–**D**). These will be briefly illustrated in the following sections.

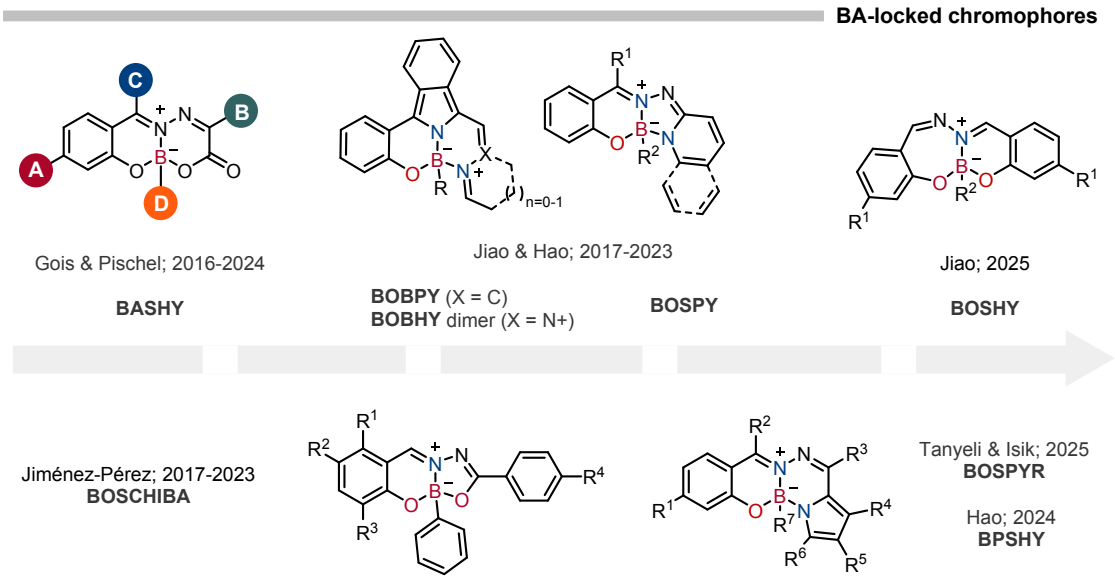

Figure 4. Selected examples of fluorescent BA-locked frameworks.

Donor component (moiety A)

Investigating the influence of the substitution at the **A** position (**Figure 4**), we observed that dyes with a stronger electron-donating *N*,*N*-diethylamino group exhibited a further red-shift in the absorbance and emission when compared to methoxy-substituted dyes; **Figure 5**.[42] For this reason, the *N*,*N*-diethylamino

View Article Online
DOI: 10.1039/D6CC00206D

group has become our prime choice for the electron-donor substituent in the structural diversification of follow-up generations of BASHY dyes.

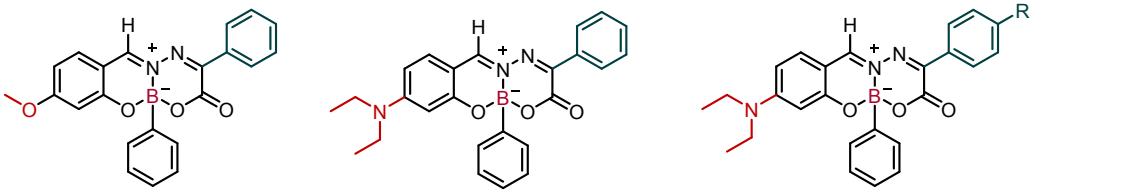

1

λ_{abs} = 420 nm; λ_f = 506 nm

2

λ_{abs} = 471 nm; λ_f = 540 nm

λ_{abs} = 476 nm; λ_f = 559 nm (**3a**; R = CF_3)
λ_{abs} = 482 nm; λ_f = 577 nm (**3b**; R = CN)
λ_{abs} = 488 nm; λ_f = 632 nm (**3c**; R = NO_2)

Figure 5. Structural variation of the donor and acceptor moiety in the BASHY platform. The maxima of the UV/vis absorption and emission spectra are provided.

Acceptor component (moiety B)

The **B** moiety (**Figure 4**), located on the opposite end of the salicylidenehydrazone backbone, was used to fine-tune the push-pull (ICT) character of BASHY dyes via introduction of electron-acceptor groups. Thus, the increasing of the electron-withdrawing properties of the phenyl *para*-substituent [Hammett constants σ_p : 0 (H; **2**), 0.54 (CF_3; **3a**), 0.66 (CN; **3b**), 0.78 (NO_2; **3c**)][60] led to a pronounced red-shift in the emission maximum of the BASHY platform (see **Figure 5**). Additionally, these fluorophores exhibited solvatofluorochromic character, with pronounced bathochromic shifts of the emission spectrum in solvents of increased polarity (**Table 1**).[61] However, this came at the cost of reduced fluorescence quantum yields. This may be reasoned with the energy-gap law, predicting a more dominant nonradiative deactivation for energetically lower lying excited singlet states. The overall solvatofluorochromic behavior corroborates the involvement of ICT in the excited singlet state of these BASHY dyes.

View Article Online
DOI: 10.1039/D6CC00206D

Table 1. Photophysical properties of **2** and **3a–c** in aerated organic solvents.

	2	**3a**	**3b**	**3c**
Toluene (P = 2.4)				
$\lambda_{abs,max}$ (nm)	471	478	484	489
$\lambda_{f,max}$ (nm)	508	516	525	535
Φ_f	0.60	0.65	0.57	0.55
THF (P = 4.0)				
$\lambda_{abs,max}$ (nm)		478	483	489
$\lambda_{f,max}$ (nm)		537	549	579
Φ_f		0.30	0.28	0.23
CH_3CN (P = 5.8)				
$\lambda_{abs,max}$ (nm)	471	476	482	488
$\lambda_{f,max}$ (nm)	540	559	577	632
Φ_f	0.08	0.05	0.05	<0.01

Initial theoretical studies of the BASHY platform, using density-functional-theory (DFT) methodology, pointed to the involvement of a pronounced ICT character of the excited state, in agreement with the observed solvatofluorochromism.[42] In a detailed follow-up theoretical study Jacquemin and co-workers confirmed the charge-transfer characteristics, but pointed out an interesting mixing with cyanine-like properties.[62] This observation prompted us to further exacerbate the cyanine-like character with the conjugative π-extension of the acceptor component (**4a–c**, **Figure 6**) and thereby to explore this photomechanistic continuum for the BASHY dye family.

View Article Online
DOI: 10.1039/D6CC00206D

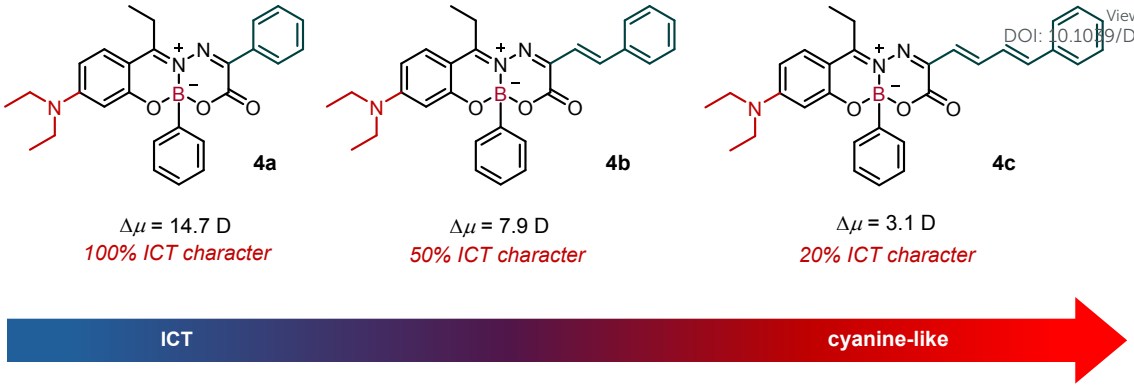

Figure 6. Dipole moment and ICT character of BASHY dyes upon π-extension of the salicylidenehydrazone ligand backbone.

In comparison to **4a**, the dyes **4b** and **4c** (**Figure 6**) feature a polymethine backbone (Cy-BASHY). These BASHY dyes display red-shifted UV/vis absorption [λ_{abs} (DMSO): **4a** – 480 nm; **4b** – 507 nm and **4c** – 525 nm] and fluorescence emission [λ_f (DMSO): **4a** – 567 nm; **4b** – 589 nm and **4c** – 599 nm], high brightness (up to 57000 $M^{-1}cm^{-1}$), significant Stokes shifts (about 80 nm), and reasonable quantum yields in highly polar solvents [Φ_f (DMSO): **4a** – 0.13; **4b** – 0.19 and **4c** – 0.24].[63] The observed dependence of the absorption and emission maxima on the π-conjugation length is in clear accordance with the theoretically expected cyanine-like character of these dyes; *cf.* König's rule.

The mapping of the increased π-extension of the salicylidenehydrazone backbone into a more significant cyanine-like character was further confirmed in DFT studies of the BASHY dyes **4a**–**c**.[64] The calculation of the D index, being the distance between the hole and electron barycenters, showed significant ICT character for **4a** (D = 3.176 Å). However, this parameter dropped gradually for **4b** (D = 1.639 Å) and indicated full cyanine-like behavior for **4c** (D = 0.639 Å).

View Article Online
DOI: 10.1039/D6CC00206D

Iminium carbon substituent (moiety C)

This substituent (moiety **C**; **Figure 4**) of the salicylidenehydrazone ligand plays a very important role in the BASHY architecture. Generally, bulkier groups at the iminium carbon confer higher hydrolytic stability to the complexes [$t_{1/2}$ in 10 mM ammonium acetate solution (pH 7): **1** – 2 min**; 5a** – 18 min; **5b** – 40 min and **5c** – 185 min] (**Figure 7**).[63]

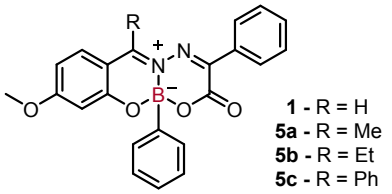

Figure 7. BASHY dyes with structural variation at the iminium carbon substituent.

In addition to the stabilization of the iminium electrophilic centre, substitution at this position with a *p*-*N*,*N*-diethylaminophenyl group (**6a**–**c**; **Figure 8**) can also induce a fluorescence quenching by photoinduced electron transfer (PeT), which can be reverted by the addition of acid in organic solvent (OFF-ON fluorescence switching; **Figure 8**). The resulting emission is observed in the green-to-orange spectral region (maxima at 520–590 nm in CH_3CN). In contrast, under physiological pH conditions (phosphate-buffered saline – PBS; pH 7), the PeT process is inherently deactivated, thereby enabling the observation of fluorescence in the red-to-NIR region (maxima at 650–680 nm).[65]

View Article Online
DOI: 10.1039/D6CC00206D

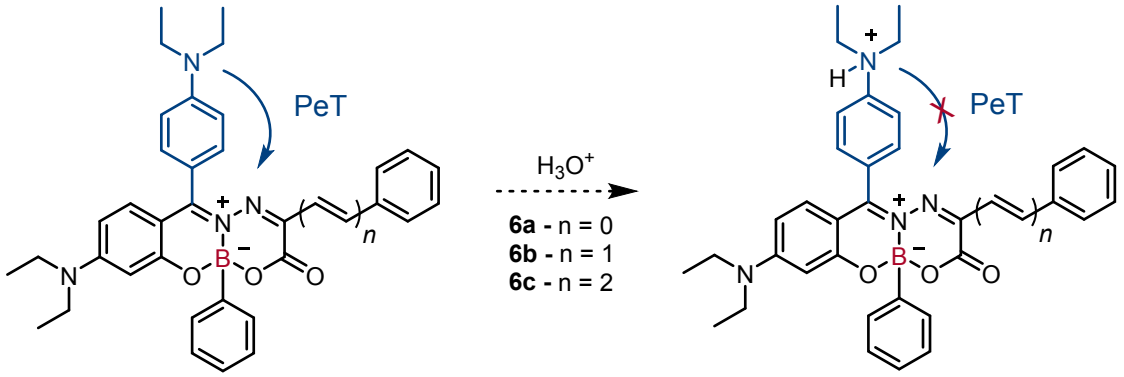

Figure 8. Fluorescence quenching of BASHY *via* PeT and re-activation under acidic conditions.

BA component (moiety D)

The BA moiety (**D** in **Figure 4**) plays a pivotal role in the BASHY architecture as the salicylidenehydrazone ligand itself is essentially non-fluorescent and it is only upon condensation with BA that the typical fluorescence of BASHY is observed. Despite this important role of the BA component as a conformational lock, the emission properties of the BASHY dyes are widely invariant with the substitution pattern of the BA aryl moiety. This appears to be direct consequence of the out-of-plane, non-conjugative orientation of the BA aryl residue, in accordance with the sp^3 character of the boron centre. This situation allows the modification of the dyes in an electronically innocent way (**Figure 9**). The preparation of dimers, (such as dye **7**) in which both halves do not communicate electronically, is one example. Thus, dye **7** retains the fluorescence properties of **2** (**Figure 5**), but the molar absorption coefficient is almost doubled [CH_3CN: 103900 $M^{-1}cm^{-1}$ (**7**) *versus* 60000 $M^{-1}cm^{-1}$ (**2**)].[42] This was confirmed by DFT calculations, which clearly confirmed that both chromophoric units feature

View Article Online
DOI: 10.1039/D6CC00206D

independent transitions, involving degenerate frontier molecular orbitals.[42] Similar conclusions were drawn from DFT calculations of a heterobichromophoric dyad featuring BASHY and BODIPY moieties (see below).[66]

Other examples are the preparation of BASHY dyes **8–10** (**Figure 9**), which were used respectively as a clickable fluorescent tag for annexin V, as a stain for astrocytes, and as a photosensitizer (PS) for photodynamic therapy (PDT); see below.[61,63,67]

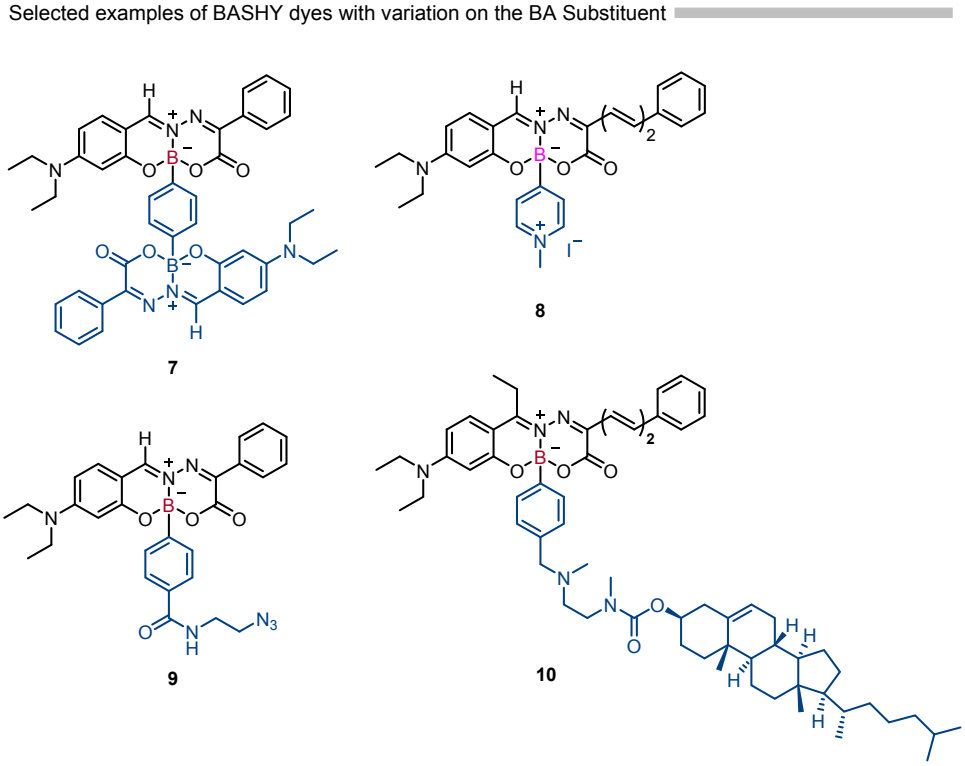

Figure 9. Examples for the structural diversification of the BA moiety, integrated in the BASHY platform.

As mentioned above, the substituent at the iminium carbon confers steric and electronic protection to this electrophilic centre, which affects the hydrolytic stability of these complexes positively. However, in order to evaluate the

View Article Online
DOI: 10.1039/D6CC00206D

hydrolytic stability of BASHY dyes in a holistic manner, including synergistic effects, we developed a multivariate linear-free energy relationship (mLFER) model.[68] For this a library of twenty structurally diverse BASHY dyes was employed. This resulted in the prediction of an optimized structure with elevated hydrolytic stability and application potential for prolonged bioimaging experiments (**Figure 10**). The identified lead structure, compound **11**, revealed remarkable stability in PBS at pH 7.4 ($t_{1/2}$ = 95 h) and in DMEM cultivation medium ($t_{1/2}$ = 128 h). Additionally, in blood plasma no measurable degradation was observed over 70 h. Interestingly, the *o*-phenyl substituent of the BA moiety was found to play a crucial role in the hydrolytic stability of this structure. DFT calculations performed on dye **11** corroborated that a steric clash between the *i*-Bu substituent at the iminium carbon and the *o*-CN phenylboronic acid component limits the nucleophilic attack of water.[68]

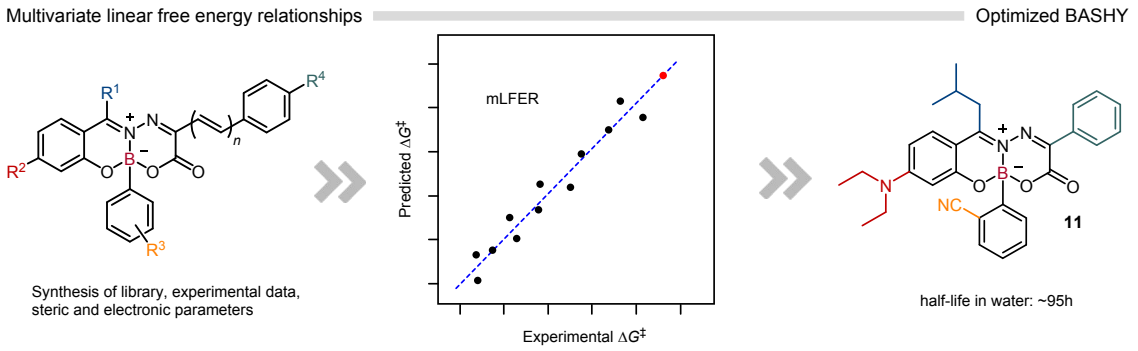

Figure 10. Workflow for the development of optimized BASHY dyes applying mLFER.

Additional Insights into the Photophysical Properties of BASHY Dyes

Based on the above outlined factors that impact the photophysical properties and the fine-tuning of the mechanistic continuum of BASHY, defined by charge-transfer and cyanine-like character, the dyes were further explored.

View Article Online
DOI: 10.1039/D6CC00206D

Two-photon-absorption (2PA) properties

A direct consequence of charge-transfer processes is the possible observation of multi-photon absorption.[69] This was verified for the series of the aforementioned dyes **2** and **3a–c** (**Figure 5**). For these dyes, 2PA between *ca.* 900 and 1000 nm was observed with cross sections (σ_2) that reached values of almost 300 GM for dye **3c** and *ca*. 200 GM for the other three dyes (**Figure 11A** and **11B**).[61] The two-photon excitation led to the population of the lowest excited singlet state, resulting in the same fluorescence as observed in conventional one-photon spectroscopy.

A

	λ_f^{2PE} (nm)	σ_2 (GM)
2	508	194 (890 nm), 117 (950 nm)
3a	518	214 (890 nm), 128 (950 nm)
3b	528	176 (890 nm), 164 (970 nm)
3c	537	283 (910 nm), 295 (980 nm)

B

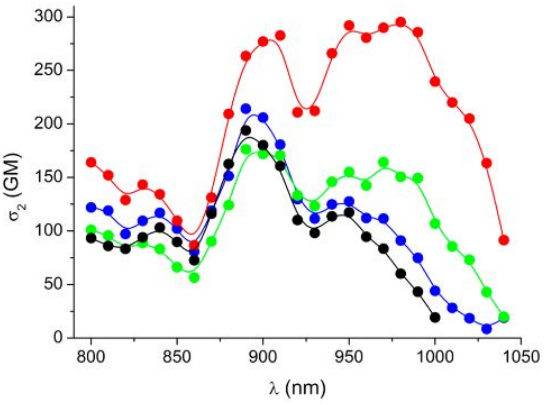

Figure 11. A) Photophysical data related to 2PA of dyes **2** and **3a–c** in toluene; **B**) 2PA spectra of the dyes **2** (black), **3a** (blue), **3b** (green), and **3c** (red) in toluene. Adapted from ref. 61 with permission from American Chemical Society, Copyright 2017.

Circularly polarized luminescence (CPL)

BASHY dyes contain a single stereogenic element, characterized by the asymmetrically substituted boron centre. Hence, the dyes are synthesized as

View Article Online
DOI: 10.1039/D6CC00206D

racemic mixtures. While the enantiomers exhibit indistinguishable photophysical properties with respect to their conventional characterization, we anticipated that they could be emitters of CPL. To demonstrate this feature, the racemates of the dyes **2** and **3a–c** (**Figure 5**) were separated by chiral chromatography and subjected to CPL measurements.[70] The observed luminescence signals coincide with the conventional fluorescence spectra, pointing to the fact that the charge-transfer features are maintained. The observed dissymmetry factors are moderate, i.e., g_{lum} *ca*. 3–5 × 10^{-4}, albeit in the order of magnitude of related organoboron dyes with similar stereogenic elements.

Energy-transfer cassettes (ETCs)

Building on the notion that BASHY dyes are efficient fluorophores, we further exploited their integration in ETCs. For this purpose, BASHY **2** was linked to a BODIPY dye (dyad **12**) *via* a phenylene spacer or a coumarin (dyad **13**) *via* a single σ-bond (**Figure 12**). For ETC **12** an efficient Förster resonance energy transfer (FRET) process (Φ_{FRET} > 0.95) was observed, with the BASHY dye being the energy donor and the BODIPY dye acting as acceptor. Indeed, upon selective excitation of the BASHY moiety (between 410 nm and 490 nm) the FRET-sensitization of the characteristic BODIPY emission (at *ca*. 580 nm) was observed. In the case of ETC **13** it is very reasonable to assume that through-bond energy transfer (TBET) is operative due to the very compact arrangement of both chromophores, this time the BASHY moiety being the energy acceptor. On excitation of **13** into the coumarin band (320 nm), BASHY emission (520 nm) was seen, implying a practically quantitative energy-transfer process (Φ_{TBET} > 0.95).[66]

View Article Online
DOI: 10.1039/D6CC00206D

Energy-transfer cassettes

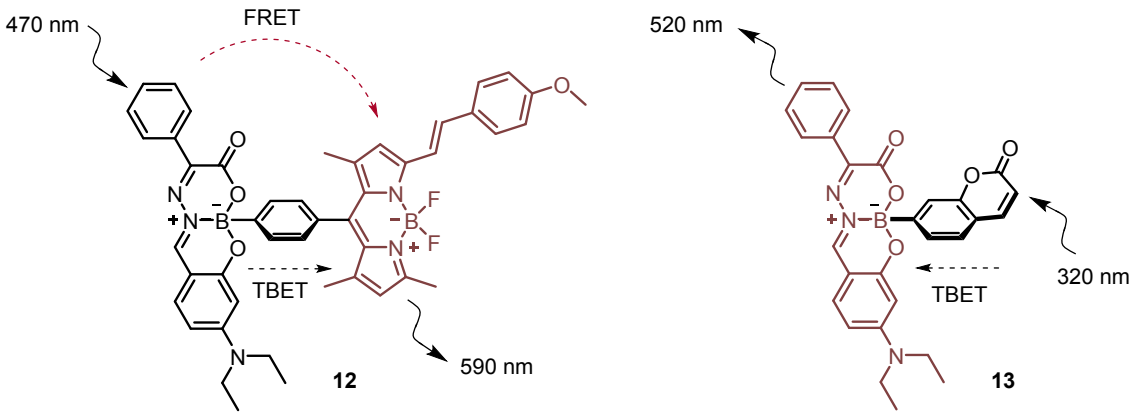

Figure 12. ETCs **12** and **13** and related mechanisms of energy transfer. Adapted from ref. 66 with permission from John Wiley and Sons, Copyright 2018.

Sensitization of singlet-oxygen ($^1O_2$) formation

For the π-extended dyes **4b** and **4c** the fluorescence quantum yields in non-polar solvents are substantially lower than for their non-extended counterpart (0.72 for dye **4a** *versus* 0.58 and 0.32 for **4b** and **4c**, respectively, in toluene; **Figure 6**). Hence, the more extended the π-conjugation system, the more competitive non-radiative pathways interfere in the excited singlet-state deactivation. A detailed study revealed that this competition consists mainly in the population of excited triplet states *via* intersystem crossing (ISC). These serve as precursors for the energy-transfer sensitized formation of $^1O_2$. As a result, especially dye **4c** is an excellent $^1O_2$ sensitizer (Φ_Δ *ca.* 0.8) in non-polar environments (**Figure 13**).[64] This provided the photophysical basis for the use of this dye in advanced applications of PDT; see below.

View Article Online
DOI: 10.1039/D6CC00206D

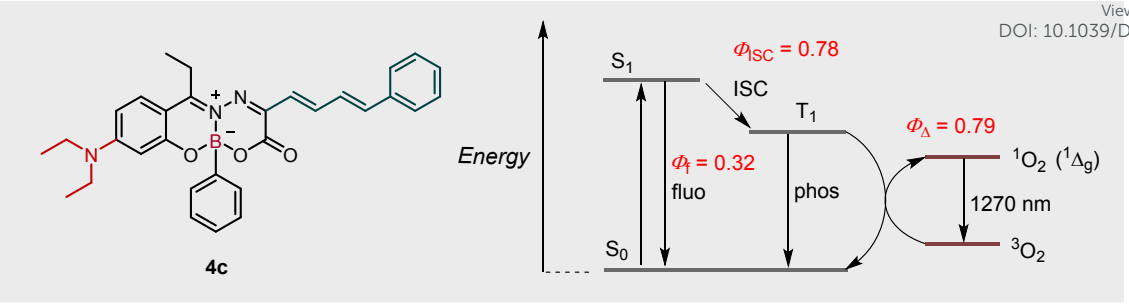

Figure 13. Proposed excited-state deactivation pathways of BASHY **4c**, including $^1O_2$ generation. Adapted from ref. 64 with permission from American Chemical Society, Copyright 2023.

Bioimaging applications of BASHY dyes

BASHY dyes are characterized by their high lipophilicity, a three-dimensional structure imposed by the sp^3-hybridized boron center, and low toxicity, as demonstrated in their incubation with healthy cell lines such as dendritic cells (DCs, JAWSII) and human retinal pigment epithelial-1 (RPE-1).[42,64] In our initial evaluation we clearly observed that the BASHY dyes **2** and **3c** (**Figure 5**) rapidly enter the cell, within just 10 minutes of incubation, and tend to accumulate in lipid droplets (LDs),[42] which are spherical cytoplasmic organelles composed of a neutral lipid core that play a key role in lipid metabolism.[71] This was established by co-localization experiments with the archetypal Nile Red stain. Throughout our studies, we never observed the labeling of the cell membrane, which we attributed to the poor ability of this highly three-dimensional structure to intercalate into a more ordered lipidic region.

Myelin debris phagocytosis by microglia during demyelination

The affinity of BASHY dyes for disordered lipid-rich regions was exploited to study microglial activity in multiple sclerosis. This condition is a demyelinating

View Article Online
DOI: 10.1039/D6CC00206D

disease of the central nervous system, characterized by the presence of demyelinated regions with accumulated myelin-lipid debris, which are cleared by microglia.[72] We observed that the BASHY dyes **2** and **4a–c** (structures in **Figure 5** and **Figure 6**) were able to label lipid debris and image the clearance in demyelinated *ex vivo* organotypic cultures and in primary microglial cells.[73] Among the tested BASHY dyes, compound **4a** exhibited superior performance, characterized by strong staining intensity and low background emission. These features enable the clear differentiation between detached myelin debris and intact or early-stage damaged myelin fibres, thereby allowing a more precise visualization of myelin clearance by lesion-associated microglial cells. In addition, BASHY **4a** facilitated the imaging of amoeboid phagocytic microglia (foamy cells) due to its efficacy in labeling myelin debris. Most importantly, BASHY **4a** was also used with an *in vivo* mice model, where the dye was found in demyelinated areas of the brain of experimental autoimmune encephalomyelitis-induced (EAE) mice (**Figure 14**).[73]

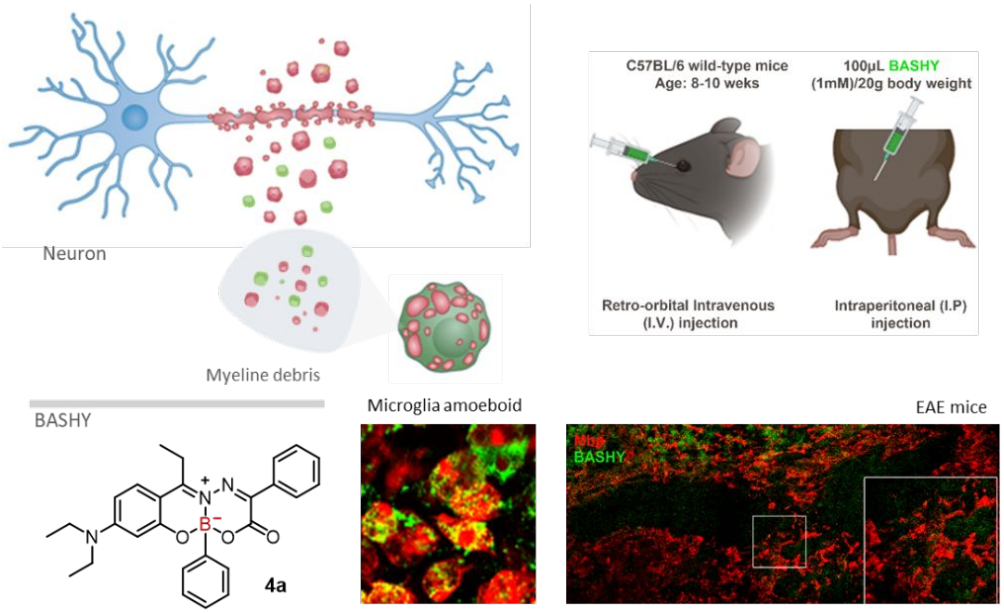

Figure 14. A) Demyelination process showing phagocytosis of BASHY-stained myelin debris by amoeboid microglia; **B**) *In vivo* evaluation of BASHY

View Article Online
DOI: 10.1039/D6CC00206D

administration in experimental autoimmune encephalomyelitis (EAE) mice. Adapted from ref. 73 under the terms and conditions of the Creative Commons Attribution (CC-BY) license, licensee MDPI, 2021.

Fluorescence lifetime imaging microscopy (FLIM)

Live-cell bioimaging is essential for understanding dynamic cellular processes in real time, providing important insights into the behavior, function, and interactions of cells in their native environment. The use of FLIM[74] is a particularly useful technique in this area, and BASHY **11** (**Figure 10**) was recently employed for this purpose in live A549 lung adenocarcinoma cells. The dye exhibits two distinct fluorescence lifetime components (τ_f), namely in vesicles (1.0 ns) and around the perinuclear region (1.9 ns). More importantly, the vesicles associated with the shorter lifetime of **11** are of particular importance in time-lapse imaging, as they have been observed to be transported within tunneling nanotubes as a form of cell-to-cell communication and content transfer.[68]

An annexin V-BASHY conjugate for the labeling of apoptotic cells

Annexin V has been widely used as a marker of apoptosis due to its ability to bind phosphatidylserine, a phospholipid membrane component, which is translocated from the inner to the outer leaflet of the plasma membrane during apoptosis. Leveraging on the modularity of the BASHY platform, the azido-substituted BASHY dye **9** (**Figure 9**) was engineered to tag annexin V *via* a strain-promoted azide-alkyne cycloaddition, resulting in the fluorescent

View Article Online
DOI: 10.1039/D6CC00206D

bioconjugate **14** (**Figure 15A**). This construct was shown to effectively label apoptotic HeLa cells (**Figure 15B**).[67]

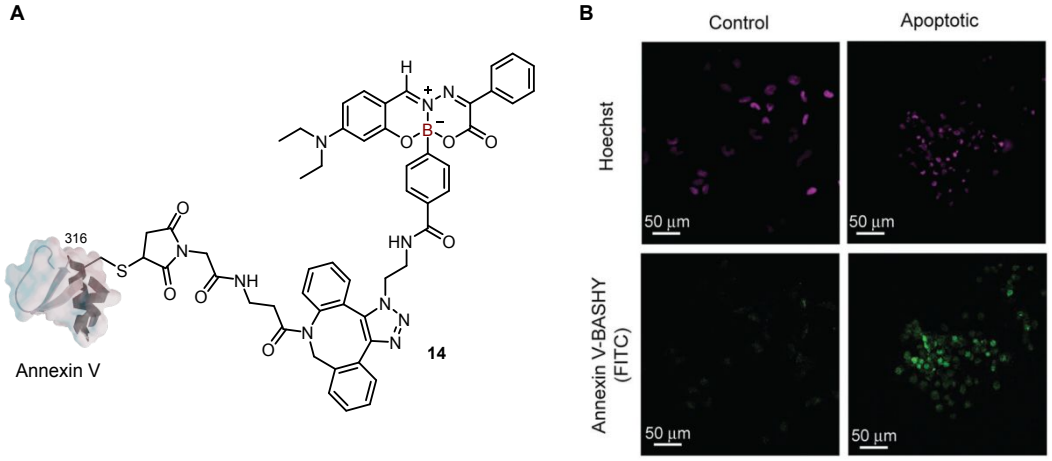

Figure 15. A) Structure of Annexin V-BASHY conjugate **14**; **B**) Confocal microscopy images of HeLa cells treated with actinomycin D (apoptotic) or with 0.1% DMSO (control), followed by incubation with Annexin V-BASHY **14** (green). Nuclear Hoechst staining (purple). Adapted from ref. 67 with permission from the Royal Society of Chemistry, Copyright 2017.

BASHY-pyridinium for the bioimaging of astrocytes

Cationic fluorophores have been shown to stain astrocytes as they express organic cation transporters that allow the transit of neurotransmitters in the brain.[75] In this study, BASHY dye **8** was engineered to contain a cationic pyridinium moiety on the BA module (**Figure 16**) in order to label organotypic cerebellar slice cultures. The slices were incubated with dye **8** and then immunostained for the astrocyte-specific glial fibrillary acidic protein (GFAP). Confocal fluorescence microscopy studies showed that dye **8** co-localized with GFAP in more than 70% of the stained area. This dye displayed a 4-fold higher co-localization with astrocytes than the non-cationic dye **15** (**Figure 16**).[63]

View Article Online
DOI: 10.1039/D6CC00206D

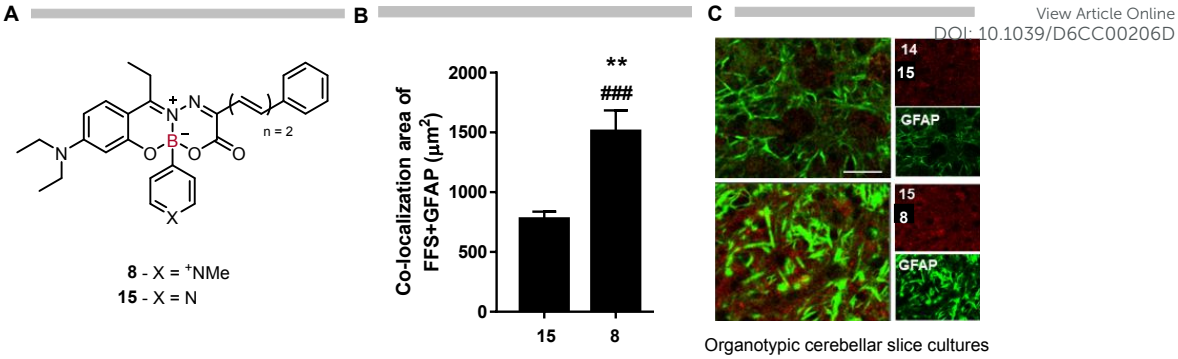

Figure 16. A) Structure of the BASHY dyes **8** (cationic) and **15** (neutral); **B**) Percentage of dye area that co-stains with GFAP; **C**) Representative images of slices stained with BASHY dyes **8** and **15** (red) and immunostained for GFAP (green). Adapted from ref. 63 with permission from John Wiley and Sons, Copyright 2020.

Therapeutic applications of the BASHY platform

Fluorescent BASHY linker for a GV1001-bortezomib conjugate

The construction of targeted drug conjugates, such antibody- or small molecule-drug conjugates is often hindered by the complexity of the linker technology, which must ensure both structural stability in circulation and controlled drug release at the target site.[76,77] Additionally, intracellular trafficking studies require bioconjugates to be fluorescent, typically by replacing the cytotoxic drug or incorporating fluorophores into the linker, both of which present drawbacks. An alternative approach is the design of inherently fluorescent linkers.[78,79] Due to the suitable bioimaging properties of BASHY dyes, this platform was re-engineered to develop fluorescent cytotoxic bioconjugates (**Figure 17**).[80]

The FDA-approved proteasome inhibitor (bortezomib; Btz), was chosen to be incorporated into the BASHY framework, while retaining the dye's photophysical properties [BASHY **4a** (λ_{abs} = 425 nm, λ_f = 504 nm, Φ_f = 0.10

View Article Online
DOI: 10.1039/D6CC00206D

versus BASHY-Btz **16** (λ_{abs} = 412 nm, λ_f = 490 nm, Φ_f = 0.02; in toluene]. Then, BASHY-Btz **16** was coupled with a cell-penetrating peptide GV1001. The resulting conjugate **17** demonstrated an improved cytoplasmic availability as verified by confocal fluorescence microscopy studies. Moreover, it exhibited improved potency against HT-29 cancer cells (IC_{50} = 100 nM) compared to non-vectorized BASHY-Btz **16** (IC_{50} = 450 nM), which showed accumulation in lipid droplets (**Figure 17**). The findings of this study revealed that the BASHY platform allows the intracellular tracking of the drug-conjugate, promotes the release of the cytotoxic cargo upon hydrolysis and elucidated the chemotherapy resistance mechanism associated with the entrapment of drugs in lipid droplets, which tend to be overexpressed in cancer cells.[80]

View Article Online
DOI: 10.1039/D6CC00206D

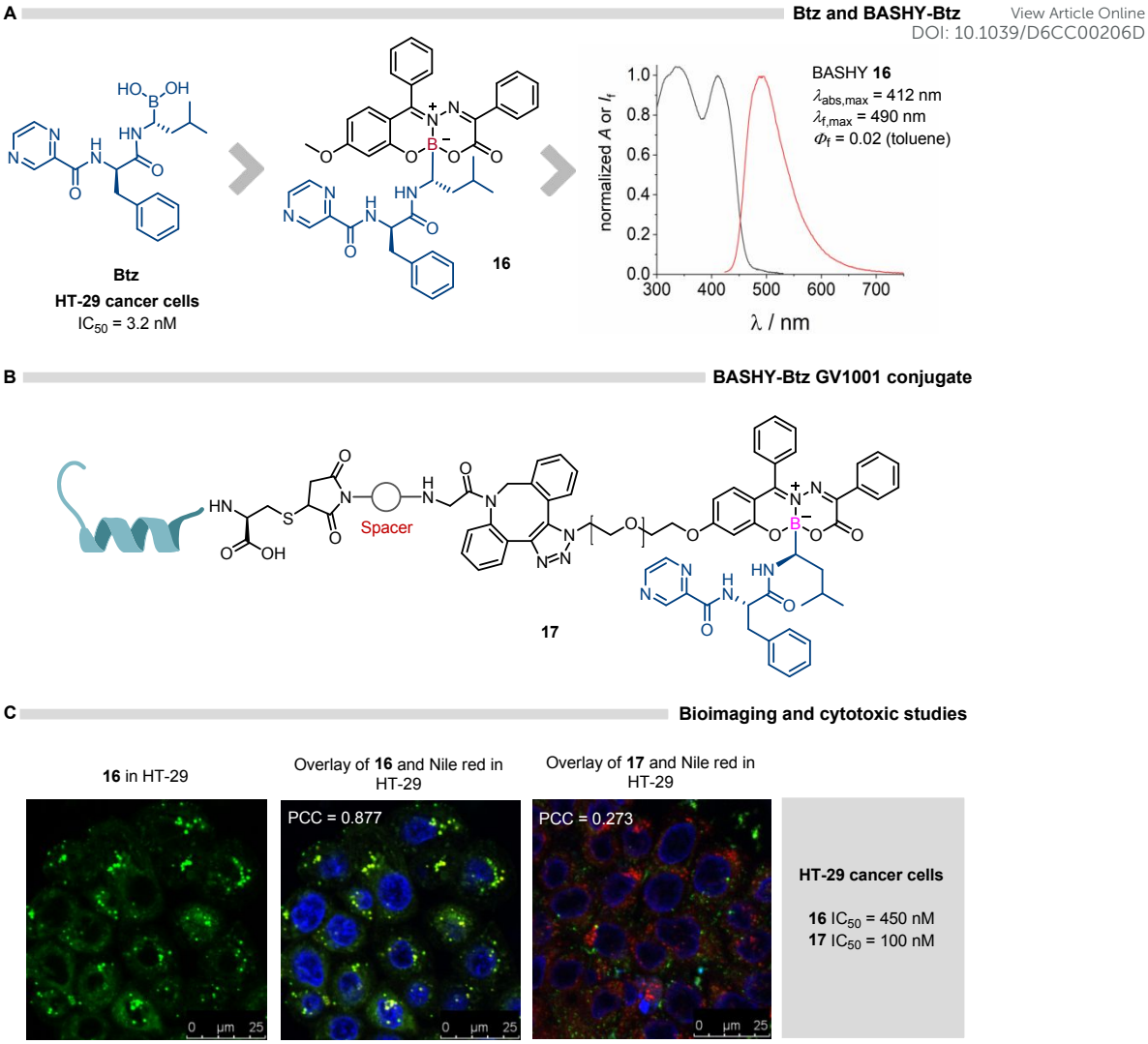

Figure 17. A) IC_{50} of Btz in HT-29 cancer cells, along with BASHY-Btz **16** structure and optical spectra (UV/vis absorption in black and fluorescence in red); **B**) Structure of the fluorescent targeted drug conjugate **17**; **C**) Cellular staining, co-localization, and cytotoxic evaluation of compounds **16** and **17** in HT-29 cancer cells. Adapted from ref. 80 with permission from American Chemical Society, Copyright 2022.

BASHY as PS platform for PDT

In oncology PDT has emerged as a promising treatment modality that uses light-sensitive compounds, known as PSs, to target and destroy malignant cells. When

View Article Online
DOI: 10.1039/D6CC00206D

activated by light of a specific wavelength, these PSs generate reactive oxygen species (ROS) that induce local cell damage.[81,82] Based on the ability of the BASHY dyes **4a–c** (**Figure 6**) and **10** (**Figure 9**) to generate $^1O_2$ upon light activation (see above), these dyes were tested as PSs for PDT.[64] BASHY **4c** revealed to be the most efficient singlet-oxygen PS [Φ_Δ – **4a** (0.23); **4b** (0.20); **4c** (0.78); in toluene] and exhibited high phototoxicity against the human glioblastoma multiform U87 cell line, with an IC_{50} value in the low nanomolar range (4.40 nM). This was accompanied by an astonishing phototoxicity index (PI > 22700). BASHY **4c** was shown to accumulate in LDs and this intracellular distribution was found to be essential for the enhanced phototoxicity and induction of ferroptosis by lipid peroxidation (LPO); **Figure 18**.[64]

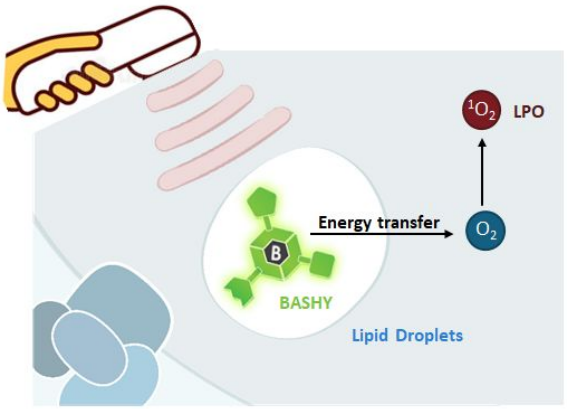

	$^{dark}IC_{50}$ (μM)	$^{light\ 540\ nm}IC_{50}$ (nM)	PI
U87 MG cell line			
4a	>100	14260 ± 780	>7
4b	>100	27.9 ± 1.5	>3600
4c	>100	4.4 ± 0.2	>22700
10	>100	98 ± 17	>1000
PPIX	4.93 ± 1.18	521 ± 94	9.5

Figure 18. BASHY as a promising PS platform for PDT that targets LDs and triggers ferroptosis. Adapted from ref. 64 with permission from American Chemical Society, Copyright 2023.

Building on the promising potency and high PI observed in cellular PDT experiments, the safety of dye **4c** was evaluated *in vivo* using zebrafish embryos (Danio rerio), a well-established toxicity model in preclinical studies.[83,84] BASHY **4c** did not display apparent dark toxicity at concentrations up to 10 μM,

View Article Online
DOI: 10.1039/D6CC00206D

in contrast to cisplatin. Subsequent PDT assays demonstrated that at 20 μM, the light-irradiation of the PS induced significant morphological abnormalities, such as heart edema, highlighting the potential of the BASHY platform for further *in vivo* phototherapeutic applications.[64]

Current limitations and potential improvements of the BASHY platform

As shown herein, in the course of our research program we have been able to engineer the BASHY platform in many aspects during the evolution of the various generations of dyes. This includes the improvement of their robustness against hydrolytic stability,[68] the further shift of their emission properties into the red spectral window (600–650 nm),[63] and the addition of stimuli-responsive functionalities.[65]

However, there is still ample room for a further evolution of the physicochemical properties related to:

a) the solubility in water (synthetic modification with potentially water-solubilizing groups, such as sulfonates or carboxylates),

b) the photostability in general and especially against the oxidation of the polymethine chain in Cy-BASHY by $^1O_2$.

c) the displacement of the emission properties into the near-infrared spectral region (>700 nm) by further extending the π-framework.

Work on these aspects is currently progressing in our research groups.

Conclusions

The inherent complexity of biological systems and the need to understand the intricate mechanisms that govern their functions have pushed the boundaries of

View Article Online
DOI: 10.1039/D6CC00206D

requirements on fluorescent dyes in modern imaging applications. As the demand for higher sensitivity, specificity, and functional adaptability grows, so does the need for innovative chromophore architectures with finely tuned photophysical properties. To address these challenges, MCRs have emerged as powerful tool for the direct and efficient generation of structurally diverse fluorophores, capable of meeting the evolving demands of advanced bioimaging technologies.

The BASHY platform is a structurally and functionally versatile class of BA-derived fluorophores with significant potential for bioimaging and therapeutic applications. Through rational design and modular synthesis, these dyes exploit the coordination of π-conjugated salicylidenehydrazone ligands to a central sp^3-hybridized boron atom, resulting in stable, three-dimensional fluorescent complexes. The most important features of BASHY dyes are their lipophilicity and suitable photostability, combined with large Stokes shifts, polarity-sensitive emission, 2PA properties and high quantum yields in non-polar environments. Furthermore, the modularity of the scaffold enables fine-tuning of photophysical properties through systematic variations of electronic structure and optimization of the hydrolytic stability. Importantly, the BA moiety in the BASHY framework allows, in most cases, structural derivatization without altering or compromising the fluorescence output. These features underscore the exceptional modularity and photophysical tunability of the BASHY platform, highlighting its potential for advanced bioimaging applications.

BASHY dyes have demonstrated considerable utility across diverse bioimaging contexts. These include selective accumulation in lipid-rich subcellular compartments such as LDs, which are overexpressed in cancer cells, labeling of astrocytes, which have a wide implication in neurochemical

View Article Online
DOI: 10.1039/D6CC00206D

processes, fluorescent tagging of apoptotic cells through bioconjugation with annexin V and targeted staining of myelin debris in models of demyelination. Notably, BASHY **4a** enabled *in vivo* imaging of demyelinated brain regions in an EAE mouse model, underpinning the translational potential of this platform in research on neuroinflammation and multiple sclerosis. The BASHY scaffold has also been adapted for advanced microscopy techniques such as FLIM, where medium-dependent lifetime enabled visualization of dynamic vesicle trafficking between cells. In addition to imaging, BASHY dyes show great promise in therapeutic applications.

BASHY derivatives demonstrated the ability to sensitize $^1O_2$ formation with high efficiency, particularly BASHY **4c**, which showed strong phototoxicity in human glioblastoma multiform U87 cell line (IC_{50} = 4.40 nM) and suitable *in vivo* safety profile in zebrafish models, validating its application in PDT.

Furthermore, the BASHY framework has been successfully integrated into a fluorescent drug conjugate, exemplified by the GV1001–BASHY–bortezomib construct (**17**). This conjugate exhibited potent cytotoxic activity against HT-29 cancer cells (IC_{50} = 100 nM), with the BASHY moiety acting simultaneously as a fluorescent tracking unit and a responsive linker, thereby enabling real-time monitoring of drug delivery.

Overall, the BASHY platform stands out as a modular chromophore technology that covers both diagnostic and therapeutic domains. Its chemical flexibility, robust fluorescence behavior, and demonstrated compatibility with cellular and *in vivo* models position BASHY dyes as promising candidates for next-generation imaging and theranostic agents.

View Article Online
DOI: 10.1039/D6CC00206D

Author contributions

F. M. F. S.: writing – original draft, review & editing. F. G. B.-C.: writing – review & editing. U. P.: funding acquisition, project administration, writing – review & editing. P. M. P. G.: funding acquisition, project administration, writing – review & editing.

Conflicts of interest

The authors declare no conflict of interest.

Acknowledgments

The authors are grateful for funding by the Spanish Ministry of Science, Innovation, and Universities (MCIU/AEI/10.13039/501100011033) and the European Regional Development Fund ERDF (grant PID2023-152556NB-I00 for U. P. and pre-doctoral contract PRE2023-001520 for F.G.B.-C.). We acknowledge funding from the Research Institute for Medicines (iMed.ULisboa) which is supported by the Fundação para a Ciência e a Tecnologia (FCT), Portuguese Agency for Scientific Research. iMed.ULisboa is funded by FCT through projects: UID/04138/2025 (https://doi.org/10.54499/UID/04138/2025); UID/PRR/04138/2025 (DOI: https://doi.org/10.54499/UID/PRR/04138/2025); UID/PRR2/04138/2025 (DOI: https://doi.org/10.54499/UID/PRR2/04138/2025). FCT is also thanked for the project grant: LISBOA2030-FEDER-00719700, DOI https://doi.org/10.54499/2023.16337.ICDT. F.M.F.S. thanks FCT for the 2021.04125.CEECIND.

View Article Online
DOI: 10.1039/D6CC00206D

References

[1] Y. Zheng, R. Cai, K. Wang, J. Zhang, Y. Zhuo, H. Dong, Y. Zhang, Y. Wang, F. Deng, E. Ji, Y. Cui, S. Fang, X. Zhang, H. Huang, K. Zhang, J. Wang, G. Li, X. Miao, Z. Wang, Y. Yang, S. Li, J. B. Grimm, K. Johnsson, E. R. Schreiter, L. D. Lavis, Z. Chen, Y. Mu and Y. Li, *Science*, 2025, **388**, eadt7705.

[2] L. Wang, M. S. Frei, A. Salim and K. Johnsson, *J. Am. Chem. Soc.*, 2019, **141**, 2770–2781.

[3] L. D. Lavis, *Biochemistry*, 2017, **56**, 5165–5170.

[4] G. Jiang, H. Liu, H. Liu, G. Ke, T. Ren, B. Xiong, X. Zhang and L. Yuan, *Angew. Chem. Int. Ed.*, 2024, **63**, e202315217.

[5] W. Xu, Z. Zeng, J.-H. Jiang, Y. Chang and L. Yuan, *Angew. Chem. Int. Ed.*, 2016, **55**, 13658–13699.

[6] A. S. Klymchenko, *Acc. Chem. Res.*, 2023, **56**, 1–12.

[7] A. S. Klymchenko, *Acc. Chem. Res.*, 2017, **50**, 366–375.

[8] A. Sharma, P. Verwilst, M. Li, D. Ma, N. Singh, J. Yoo, Y. Kim, Y. Yang, J. Zhu, H. Huang, X. Hu, X. He, L. Zeng, T. D. James, X. Peng, J. L. Sessler and J. S. Kim, *Chem. Rev.*, 2024, **124**, 2699–2804.

[9] Y. Tanaka, M. Taki and S. Yamaguchi, *Chem. Commun.*, 2025, **61**, 1164–1167.

[10] M. Hirai, N. Tanaka, M. Sakai and S. Yamaguchi, *Chem. Rev.*, 2019, **119**, 8291–8331.

[11] X. Liu and Y. Chang, *Chem. Soc. Rev.*, 2022, **51**, 1573–1591.

[12] S. Munan, Y. Chang and A. Samanta, *Chem. Commun.*, 2024, **60**, 501–521.

[13] C. Lim, D. Seah and M. Vendrell, *Chem. Soc. Rev.*, 2026, **55**, 1352–1370.

[14] S. Benson, F. de Moliner, W. Tipping and M. Vendrell, *Angew. Chem. Int. Ed.*, 2022, **61**, e202204788.

View Article Online
DOI: 10.1039/D6CC00206D

[15] F. de Moliner, N. Kielland, R. Lavilla, M. Vendrell, *Angew. Chem. Int. Ed.*, 2017, **56**, 3758–3769.

[16] G. Hong, A. L. Antaris and H. Dai, *Nat. Biomed. Eng.*, 2017, **1**, 0010.

[17] K. Grover, A. Koblova, A. T. Pezacki, C. J. Chang and E. J. New, *Chem. Rev.*, 2024, **124**, 5846–5929.

[18] J. H. Choi, S. Kim, O. Kang, S. Y. Choi, J. Y. Hyun, H. S. Lee and I. Shin, *Chem. Soc. Rev.*, 2024, **53**, 9446–9489.

[19] L. D. Lavis and R. T. Raines, *ACS Chem. Biol.*, 2014, **9**, 855–866.

[20] J. V. Jun, D. M. Chenoweth and E. J. Petersson, *Org. Biomol. Chem.*, 2020, **18**, 5747–5763.

[21] L. Levi and T. J. J. Müller, *Chem. Soc. Rev.*, 2016, **45**, 2825–2846.

[22] L. Brandner and T. J. J. Müller, *Front. Chem.*, 2023, **11**, 1124209.

[23] I. Saridakis, M. Riomet, O. J. V. Belleza, G. Coussanes, N. K. Singer, N. Kastner, Y. Xiao, E. Smith, V. Tona, A. de la Torre, E. F. Lopes, P. A. Sánchez-Murcia, L. González, H. H. Sitte and N. Maulide, *Angew. Chem. Int. Ed.*, 2024, **63**, e202318127.

[24] A. Loudet and K. Burgess, *Chem. Rev.*, 2007, **107**, 4891–4932.

[25] D. Frath, J. Massue, G. Ulrich and R. Ziessel, *Angew. Chem. Int. Ed.*, 2014, **53**, 2290–2310.

[26] A. M. Comiskey and E. V. Anslyn, *J. Org. Chem.*, 2025, **90**, 7161–7167.

[27] R. R. Groleau, T. D. James and S. D. Bull, *Coord. Chem. Rev.*, 2021, **428**, 213599.

[28] H. Reyes, B. M. Muñoz, N. Farfán, R. Santillan, S. Rojas-Lima, P. G. Lacroix and K. Nakatani, *J. Mater. Chem.*, 2002, **12**, 2898–2903.

[29] R. Chan-Navarro, V. M. Jiménez-Pérez, B. M. Muñoz-Flores, H. V. R. Dias, I. Moggio, E. Arias, G. Ramos-Ortíz, R. Santillan, C. García, M. E. Ochoa, M. Yousufuddin and N. Waksman, *Dyes Pigm.*, 2013, **99**, 1036–1043.

[30] D. G. Hall, *Boronic Acids - Preparation and Applications in Organic Synthesis, Medicine and Materials*, Wiley-VCH Verlag & Co. KGaA, Weinheim, 2011.

[31] S. D. Bull, M. G. Davidson, J. M. H. van den Elsen, J. S. Fossey, A. T. A. Jenkins, Y. Jiang, Y. Kubo, F. Marken, K. Sakurai, J. Zhao and T. D. James, *Acc. Chem. Res.*, 2013, **46**, 312–326.

[32] D. Wu, A. C. Sedgwick, T. Gunnlaugsson, E. U. Akkaya, J. Yoon and T. D. James, *Chem. Soc. Rev.*, 2017, **46**, 7105–7123.

[33] R. Nishiyabu, Y. Kubo, T. D. James and J. S. Fossey, *Chem. Commun.*, 2011, **47**, 1106–1123.

[34] Y. Kubo, A. Kobayashi, T. Ishida, Y. Misawa and T. D. James, *Chem. Commun.*, 2005, 2846–2848.

[35] H. Reyes, J. M. Rivera, N. Farfán, R. Santillan, P. G. Lacroix, C. Lepetit and K. Nakatani, *J. Organomet. Chem.*, 2005, **690**, 3737–3745.

[36] J. F. Lamère, P. G. Lacroix, N. Farfán, J. M. Rivera, R. Santillan and K. Nakatani, *J. Mater. Chem.*, 2006, **16**, 2913–2920.

[37] B. M. Muñoz, R. Santillan, M. Rodríguez, J. M. Méndez, M. Romero, N. Farfán, P. G. Lacroix, K. Nakatani, G. Ramos-Ortíz and J. L. Maldonado, *J. Organomet. Chem.*, 2008, **693**, 1321–1334.

[38] M. Rodríguez, G. Ramos-Ortíz, M. I. Alcalá-Salas, J. L. Maldonado, K. A. López-Varela, Y. López, O. Domínguez, M. A. Meneses-Nava, O. Barbosa-García, R. Santillan and N. Farfán, *Dyes Pigm.*, 2010, **87**, 76–83.

View Article Online
DOI: 10.1039/D6CC00206D

[39] J. Su, F. Chen, V. L. Cryns and P. B. Messersmith, *J. Am. Chem. Soc.*, 2011, **133**, 11850–11853.

[40] J. P. M. António, R. Russo, C. Parente Carvalho, P. M. S. D. Cal and P. M. P. Gois, *Chem. Soc. Rev.*, 2019, **48**, 3513–3536.

[41] J. P. M. António, I. L. Roque, F. M. F. Santos and P. M. P. Gois, *Acc. Chem. Res.*, 2025, **58**, 673–687.

[42] F. M. F. Santos, J. N. Rosa, N. R. Candeias, C. Parente Carvalho, A. I. Matos, A. E. Ventura, H. F. Florindo, L. C. Silva, U. Pischel and P. M. P. Gois, *Chem. Eur. J.*, 2016, **22**, 1631–1637.

[43] W. Dou, H. Han, A. C. Sedgwick, G. Zhu, Y. Zang, X. Yang, J. Yoon, T. D. James, J. Li and X. He, *Sci. Bull.*, 2022, **67**, 853–878.

[44] X. Wang, Q. Ding, R. R. Groleau, L. Wu, Y. Mao, F. Che, O. Kotova, E. M. Scanlan, S. E. Lewis, P. Li, B. Tang, T. D. James and T. Gunnlaugsson, *Chem. Rev.*, 2024, **124**, 7106–7164.

[45] N. Chen, W. Zhang, S. Chen, Q. Wu, C. Yu, Y. Wei, Y. Xu, E. Hao and L. Jiao, *Org. Lett.*, 2017, **19**, 2026–2029.

[46] J. Wang, X. Fang, X. Guo, Q. Wu, Q. Gong, C. Yu, E. Hao and L. Jiao, *Org. Lett.*, 2021, **23**, 4796–4801.

[47] M. Ibarra-Rodríguez, B. M. Muñoz-Flores and V. M. Jiménez-Pérez, *J. Lumin.*, 2018, **198**, 342–349.

[48] M. Ibarra-Rodríguez, B. M. Muñoz-Flores, R. Chan-Navarro, N. Waksman, A. Saucedo-Yañez, M. Sánchez and V. M. Jiménez-Pérez, *Opt. Mater.*, 2019, **89**, 123–131.

[49] M. López-Espejel, M. Ibarra-Rodríguez, B. M. Muñoz-Flores, M. R. Bahena-Villarreal, A. A. Cavazos-Jaramillo, M. D. Garza-Villegas, C. Rodríguez-

Padilla, I. E. Luna-Cruz, H. V. R. Dias, J. M. Alcocer-González and V. M. Jiménez-Pérez, *New J. Chem.*, 2023, **47**, 7975–7985.

[50] C. Yu, G. Di, Q. Li, X. Guo, L. Wang, Q. Gong, Y. Wei, Q. Zhao, L. Jiao and E. Hao, *Inorg. Chem.*, 2024, **63**, 21397–21409.

[51] L. Wang, Y. Sun, C. Yu, W. Ma, Y. Shang, L. Ding, T. Wang, X. Guo, J. Zhang, Y. Li, E. Hao, G. Wang and L. Jiao, *Org. Lett.*, 2025, **27**, 8551–8556.

[52] M. Ibarra-Rodríguez, B. M. Muñoz-Flores, H. V. R. Dias, M. Sánchez, A. Gomez-Treviño, R. Santillan, N. Farfán and V. M. Jiménez-Pérez, *J. Org. Chem.*, 2017, **82**, 2375–2385.

[53] M. Ibarra-Rodríguez, B. M. Muñoz-Flores, A. Gómez-Treviño, R. Chan-Navarro, J. C. Berrones-Reyes, A. Chávez-Reyes, H. V. R. Dias, M. Sánchez Vázquez and V. M. Jiménez-Pérez, *Appl. Organomet. Chem.*, 2019, **33**, e4718.

[54] J. Jia and J. Wen, *Tetrahedron Lett.*, 2021, **71**, 153006.

[55] E. B. Kömüşdoğan, S. Batool, E. Şahin, E. Yildirim, M. Işık and C. Tanyeli, *Chem. Commun.*, 2025, **61**, 576–579.

[56] B. Tharmalingam, R. Kishore Kumar, O. Anitha, W. Kaminsky, J. G. Malecki and B. Murugesapandian, *Dalton Trans.*, 2025, **54**, 3897–3910.

[57] S. Guieu, C. I. C. Esteves, J. Rocha and A. M. S. Silva, *Molecules*, 2020, **25**, 6039.

[58] H. Wang, X. Guo, W. Bu, Z. Kang, C. Yu, Q. Wu, L. Jiao and E. Hao, *Dyes Pigm.*, 2023, **210**, 111013.

[59] V. Savickienė, A. Bieliauskas, S. Belyakov, E. Arbačiauskienė and A. Šačkus, *Molecules*, 2024, **29**, 3432.

[60] D. H. McDaniel and H. C. Brown, *J. Org. Chem.*, 1958, **23**, 420–427.

View Article Online
DOI: 10.1039/D6CC00206D

[61] M. M. Alcaide, F. M. F. Santos, V. F. Pais, J. I. Carvalho, D. Collado, E. Pérez-Inestrosa, J. F. Arteaga, F. Boscá, P. M. P. Gois and U. Pischel, *J. Org. Chem.*, 2017, **82**, 7151–7158.

[62] A. D. Laurent, B. Le Guennic and D. Jacquemin, *Theor. Chem. Acc.*, 2016, **135**, 173.

[63] F. M. F. Santos, Z. Domínguez, J. P. L. Fernandes, C. Parente Carvalho, D. Collado, E. Pérez-Inestrosa, M. V. Pinto, A. Fernandes, J. F. Arteaga, U. Pischel and P. M. P. Gois, *Chem. Eur. J.*, 2020, **26**, 14064–14069.

[64] M. J. S. A. Silva, Y. Zhang, R. Vinck, F. M. F. Santos, J. P. M. António, L. Gourdon-Grünewaldt, C. Zaouter, A. Castonguay, S. A. Patten, K. Cariou, F. Boscá, F. Nájera, J. F. Arteaga, G. Gasser, U. Pischel and P. M. P. Gois, *Bioconjugate Chem.*, 2023, **34**, 2337–2344.

[65] J. Felicidade, F. M. F. Santos, J. F. Arteaga, P. Remón, R. Campos-González, H. Nguyen, F. Nájera, F. Boscá, D. Y. W. Ng, P. M. P. Gois and U. Pischel, *Chem. Eur. J.*, 2023, **29**, e202300579.

[66] F. M. F. Santos, Z. Domínguez, M. M. Alcaide, A. I. Matos, H. F. Florindo, N. R. Candeias, P. M. P. Gois and U. Pischel, *ChemPhotoChem*, 2018, **2**, 1038–1045.

[67] P. M. S. D. Cal, F. Sieglitz, F. M. F. Santos, C. Parente Carvalho, A. Guerreiro, J. B. Bertoldo, U. Pischel, P. M. P. Gois and G. J. L. Bernardes, *Chem. Commun.*, 2017, **53**, 368–371.

[68] J. M. J. M. Ravasco, J. Felicidade, M. V. Pinto, F. M. F. Santos, R. Campos-González, J. F. Arteaga, M. Mehraz, C. Langevin, A. Fernandes, H. Nguyen, D. Y. W. Ng, J. A. S. Coelho, U. Pischel and P. M. P. Gois, *JACS Au*, 2024, **4**, 4212–4222.

[69] M. Pawlicki, H. A. Collins, R. G. Denning and H. L. Anderson, *Angew. Chem. Int. Ed.*, 2009, **48**, 3244–3266.

[70] V. G. Jiménez, F. M. F. Santos, S. Castro-Fernández, J. M. Cuerva, P. M. P. Gois, U. Pischel and A. G. Campaña, *J. Org. Chem.*, 2018, **83**, 14057–14062.

[71] A. Zadoorian, X. Du and H. Yang, *Nat. Rev. Endocrinol.*, 2023, **19**, 443–459.

[72] K. M. Monroe and G. Di Paolo, *Nat. Neurosci.*, 2021, **24**, 451–452.

[73] M. V. Pinto, F. M. F. Santos, C. Barros, A. R. Ribeiro, U. Pischel, P. M. P. Gois and A. Fernandes, *Cells,* 2021, **10**, 3163.

[74] B. Torrado, B. Pannunzio, L. Malacrida and M. A. Digman, *Nat. Rev. Methods Primers*, 2024, **4**, 80.

[75] A. N. Preston, J. D. Farr, B. K. O'Neill, K. K. Thompson, S. E. Tsirka and S. T. Laughlin, *ACS Chem. Biol.*, 2018, **13**, 1493–1498.

[76] V. Kostova, P. Désos, J. Starck and A. Kotschy, *Pharmaceuticals*, 2021, **14**, 442.

[77] J. D. Bargh, A. Isidro-Llobet, J. S. Parker and D. R. Spring, *Chem. Soc. Rev.*, 2019, **48**, 4361–4374.

[78] B. Lee, C. Chalouni, S. Doll, S. C. Nalle, M. Darwish, S. P. Tsai, K. R. Kozak, G. Del-Rosario, S. Yu, H. Erickson and R. Vandlen, *Bioconjugate Chem.*, 2018, **29**, 2468–2477.

[79] D. Xiao, L. Zhao, F. Xie, S. Fan, L. Liu, W. Li, R. Cao, S. Li, W. Zhong and X. Zhou, *Theranostics*, 2021, **11**, 2550–2563.

[80] S. Baldo, P. Antunes, J. F. Felicidade, F. M. F. Santos, J. F. Arteaga, F. Fernandes, U. Pischel, S. N. Pinto and P. M. P. Gois, *ACS Med. Chem. Lett.*, 2022, **13**, 128–133.

View Article Online
DOI: 10.1039/D6CC00206D

[81] D. E. J. G. J. Dolmans, D. Fukumura and R. K. Jain, *Nat. Rev. Cancer*, 2003, **3**, 380–387.

[82] T. Mishchenko, I. Balalaeva, A. Gorokhova, M. Vedunova and D. V. Krysko, *Cell Death Dis.*, 2022, **13**, 455.

[83] F. M. Richards, W. K. Alderton, G. M. Kimber, Z. Liu, I. Strang, W. S. Redfern, J. Valentin, M. J. Winter and T. H. Hutchinson, *J. Pharmacol. Toxicol. Methods*, 2008, **58**, 50–58.

[84] N. Mandrekar and N. L. Thakur, *Biotechnol. Lett.*, 2009, **31**, 171–179.

View Article Online
DOI: 10.1039/D6CC00206D

BASHY dyes as modular chromophores for multifaceted biorelevant applications: From imaging to photodynamic therapy

Fábio M. F. Santos,*[a] Francisco G. Blandón-Cumbreras,[b] Uwe Pischel*[b] and Pedro M. P. Gois*[a]

[a] *Research Institute for Medicines (iMed.ULisboa), Faculty of Pharmacy, Universidade de Lisboa, Lisbon 1649-003, Portugal*

[b] *CIQSO – Centre for Research in Sustainable Chemistry and Department of Chemistry, University of Huelva, Campus de El Carmen, E-21071 Huelva, Spain*

Data Availability Statement

View Article Online
DOI: 10.1039/D6CC00206D

This Feature Article did not generate or analyse any new experimental or computational data.